

Quantification of myoglobin deoxygenation and intracellular partial pressure of O₂ during muscle contraction during haemoglobin-free medium perfusion

著者	Takakura Hisashi, Masuda Kazumi, Hashimoto Takeshi, Iwase Satoshi, Jue Thomas
journal or publication title	Experimental Physiology
volume	95
number	5
page range	630-640
year	2010-05-01
URL	http://hdl.handle.net/2297/24446

doi: 10.1113/expphysiol.2009.050344

1 **Abstract**

2

3

4

5

6

7

8

9

10

11

12

13

14

15

16

17

18

19

Although the O₂ gradient regulates O₂ flux from the capillary into the myocyte to meet the energy demands of contracting muscle, intracellular O₂ dynamics during muscle contraction remain unclear. Our hindlimb perfusion model allows the determination of intracellular myoglobin (Mb) saturation (S_{mb}O₂) and intracellular oxygen tension of myoglobin (P_{mb}O₂) in contracting muscle using near infrared spectroscopy (NIRS). The hindlimb of male Wistar rats was perfused from the abdominal aorta with a well-oxygenated hemoglobin (Hb)-free Krebs-Henseleit buffer. The deoxygenated Mb (Δ [deoxy-Mb]) signal was monitored by NIRS. Based on the value of Δ [deoxy-Mb], S_{mb}O₂ and P_{mb}O₂ were calculated and the time course was evaluated by an exponential function model. Both S_{mb}O₂ and P_{mb}O₂ started to decrease immediately after the onset of contraction. The steady state values of S_{mb}O₂ and P_{mb}O₂ progressively decreased with relative work intensity or muscle oxygen consumption. At the maximal twitch rate, S_{mb}O₂ and P_{mb}O₂ were 49% and 2.4 mmHg, respectively. Moreover, the Mb O₂ release rate at the onset of contraction increased with muscle oxygen consumption. These results suggest that at the onset of muscle contraction, Mb supplies O₂ during the steep decline in P_{mb}O₂, which expands the O₂ gradient to increase the O₂ flux to meet the increased energy demands.

1 **Abbreviations**

2

3 CO, carbon monoxide; DO_2 , O_2 diffusion conductance; 1H -MRS, 1H -magnetic resonance
4 spectroscopy; Hb, hemoglobin; Mb, myoglobin; $m\dot{V}O_2$, muscle oxygen consumption; $\Delta m\dot{V}O_2$,
5 the change in $m\dot{V}O_2$ from the resting value; NIRS, near infrared spectroscopy; PO_2 , oxygen
6 tension; $P_{mb}O_2$, intracellular oxygen tension; $P_{cap}O_2$, microvascular oxygen tension; $S_{mb}O_2$,
7 oxygen saturation of myoglobin; $\Delta[\text{deoxy-Mb}]$, changes in the NIRS signal associated with
8 the concentration of deoxygenated Mb; $\Delta[\text{oxy-Mb}]$, changes in the NIRS signal associated
9 with the concentration of oxygenated Mb; BL, the baseline value; AP, the amplitude between
10 BL and the steady-state value component; $_{0.63}AP/MRT$, the mean rate of change to 63% of the
11 AP value; TD, the time delay between the start of contraction and the appearance of the $P_{mb}O_2$
12 and $S_{mb}O_2$ signal; τ , the exponential time constant of the kinetics of the $P_{mb}O_2$ and $S_{mb}O_2$;
13 MRT, the mean response time of the kinetics that equals $TD + \tau$.

1 **Introduction**

2

3 Cellular respiration is influenced by a wide range of mechanisms including the
4 response of the cardiovascular and metabolic systems to meet the changing energy demands
5 in muscle. Although the O₂ gradient between the microvasculature and myocyte is particularly
6 important for O₂ diffusion to sustain cellular respiration in contracting muscle, intracellular O₂
7 dynamics during muscle contraction remain unknown.

8 A phosphorescence quenching technique has sometimes been used to determine
9 microvascular oxygen tension (P_{cap}O₂) in contracting muscle (Behnke *et al.* 2001;
10 McDonough *et al.* 2005). In healthy rodent skeletal muscle, the P_{cap}O₂ decreased
11 exponentially at the onset of 1 Hz contractions with an approximate 20 sec time delay
12 (Behnke *et al.* 2001). In contrast, the estimated muscle oxygen consumption (m \dot{V} O₂)
13 calculated from capillary red blood cell flux and P_{cap}O₂ increased immediately after onset of
14 the muscle contraction. A change in m \dot{V} O₂ without a corresponding change in P_{cap}O₂ would
15 imply an increased O₂ diffusing capacity (DO₂), according to Fick's law. However, the study
16 did not measure a key parameter, the kinetics of P_{mb}O₂ (Behnke *et al.* 2002; Poole *et al.* 2007).
17 Without a P_{mb}O₂ dynamics measurement, defining the limiting factor as DO₂ at the onset of
18 exercise remains debatable.

19 The P_{mb}O₂ during exercise can play a key role in regulating the \dot{V} O₂ in exercising
20 muscle (Molé *et al.* 1999). In order for O₂ delivery from capillaries to mitochondria to
21 increase to accommodate the increasing oxygen demand, P_{mb}O₂ should fall so as to increase
22 the O₂ gradient from the capillary to the muscle cell during exercise. In fact, ¹H-magnetic
23 resonance spectroscopy (¹H-MRS) experiments have shown an increasing signal intensity of
24 deoxy-Mb His F8 N_δH during contraction in human leg muscle, suggesting a fall in
25 intracellular PO₂ (Molé *et al.* 1999; Richardson *et al.* 1995). However, while Richardson *et al.*

1 (1995) have reported that Mb does not desaturate in proportion to increased work output,
2 Molé *et al.* (1999) have shown that Mb becomes increasingly desaturated with increasing
3 oxygen consumption or power output during progressive plantar flexion exercise. Moreover,
4 Molé *et al.* (1999) indicate that $P_{mb}O_2$ can modulate the O_2 gradient. The discrepancy between
5 the two studies may originate from differences in the muscle group studied, the subject
6 population, and/or the MRS acquisition/processing methodology.

7 Near infrared spectroscopy (NIRS) can investigate the dynamics of tissue
8 oxygenation in contracting muscle during the transition from rest to work with high time
9 resolution, if it can discriminate the Mb from the Hb interference. Indeed, NIRS measurement
10 allows detection of the Mb desaturation kinetics under Hb-free buffer perfused conditions,
11 indicating a significant contribution of signals derived from Mb to the NIRS signal and
12 progressive desaturation of Mb with work intensity (Masuda *et al.* 2010).

13 The present study utilizes NIRS to investigate Mb desaturation and $P_{mb}O_2$ kinetics
14 during muscle contraction at different work and intensity or $m\dot{V}O_2$ levels. Mb desaturates
15 immediately at the onset of contraction, which reflects a steep decline in the $P_{mb}O_2$ and a
16 sudden widening of the O_2 gradient changes to meet the increased metabolic demand.
17 Moreover, $P_{mb}O_2$ progressively decreases as contraction force and $m\dot{V}O_2$ increase.

18

19

20 **Materials and Methods**

21

22 *Experimental Animals and Preparation of Hindlimb Perfusion*

23 All experimental procedures performed in the present study conformed to the
24 Fundamental Guidelines for Proper Conduct of Animal Experiment and Related Activities in
25 Academic Research Institutions (Published by the Ministry of Education, Culture, Sports,

1 Science and Technology. Japan) and was approved by the ethics committee for Animal
2 Experimentation of Kanazawa University (Protocol#: AP-080943).

3 Male Wistar rats (9 weeks old, 257-295 g body weight, n = 6) were used for the
4 experiments in this study. All rats were housed in a temperature-controlled room at 23 ± 2 °C
5 with a light-dark cycle of 12 h and maintained on a commercial diet with water ad libitum.

6 All surgical procedures were performed under pentobarbital sodium anesthesia (45
7 mg/kg intraperitoneal). Physiological body temperature was maintained using a heated mat.
8 Preparation of isolated rat hindlimb and the perfusion apparatus were described in a previous
9 report (Masuda *et al.* 2010). In brief, the abdominal wall was first incised from the pubic
10 symphysis to the xiphoid process. The spermatic, testis, and inferior mesenteric arteries and
11 veins were ligated, and the spermatic, the testes, and part of the descending colon were
12 excised, together with contiguous adipose tissue. The caudal artery and internal iliac artery
13 and vein were also ligated. Ligatures were placed around the neck of the bladder, the anterior
14 prostate and the prostate gland. The vessels that supply the subcutaneous region were also
15 ligated. Following these ligations, the inferior epigastric, iliolumbar and renal arteries and
16 veins were ligated as well as the coeliac axis and portal vein. A further ligature was placed
17 around the tail. After the euthanasia by injection of 1M KCl solution into the heart, an Hb-free
18 Krebs-Henseleit buffer (NaCl, 118 mM; KCl, 5.9 mM; KH_2PO_4 , 1.2 mM; MgSO_4 , 1.2 mM;
19 CaCl_2 , 1.8 mM; NaHCO_3 , 20mM; Glucose, 15 mM) was perfused into the abdominal aorta in
20 a flow-through mode at a constant flow.

21 The flow rate was set to 22 ml/min corresponding to a perfusion pressure of around
22 90 mmHg, based on the methods reported by Shiota and Sugano (1986). In the present study,
23 average perfusion pressure was 88.7 ± 3.7 mmHg when the flow rate was set at 22 ml/min.
24 Therefore, the perfusion resistance (ml/min/mmHg) was also unchanged throughout the
25 perfusion period (4.0 ± 0.1 ml/min/mmHg). Besides, no symptom of edema in the hindlimb

1 was confirmed at the given flow rate. After cannulating into the abdominal aorta, the
2 contralateral (right hindlimb) common iliac artery was ligated. The Krebs-Henseleit buffer
3 containing Heparin (1000 U/l) was perfused into the hindlimb for 10 min from the beginning
4 of the perfusion to prevent clotting of the blood and to wash out blood from the hindlimb.

5 The perfusate and the muscle temperature were maintained at 37 °C. The rat
6 hindlimb was perfused with buffer equilibrated with 95%O₂ + 5%CO₂ for 30 min before and
7 throughout the exercise protocol. The presence of CO₂ maintained the pH between 7.3-7.4.
8 The effluent was collected from the inferior vena cava in order to measure the $\dot{m}V\dot{O}_2$ and the
9 concentration of lactate and pyruvate.

10

11 *Twitch Contraction Protocol*

12 The buffer was equilibrated for 30 min from the beginning of the perfusion
13 experiments. The sciatic nerve of the left hindlimb was then exposed and connected to two
14 parallel stainless steel wire electrodes (Unique Medical, Tokyo, Japan) and the Achilles'
15 tendon was connected to a sensitive strain gauge with a string (MLT500/D, AD Instrument,
16 Castle Hill, NSW, Australia). Slack in the string was removed by several brief tetanic
17 contractions. To elicit a series of isometric twitch contractions, electric stimuli were delivered
18 to the muscle at its optimum length, at which the muscle generated peak tension, via stainless
19 electrodes on the sciatic nerve. The stimulation consisted of a single square wave (delay: 10
20 μ sec, duration: 1 msec) controlled by an electro stimulator system (Model RU-72, Nihon
21 Koden, Tokyo, Japan). The stimulation was 1 Hz of frequency for 120 sec (120 twitch
22 contractions). The target tension was controlled by changing the voltage of the stimuli to
23 obtain 50~100% of peak tension under buffer-perfused conditions (3-8 volts). The twitch
24 tension was calculated as the average of a series of contractions. Increasing the stimulation
25 voltage in order to increase the force of contraction recruits nerve fibers that are closest to the

1 stimulating electrodes, and in reverse order with large neurons supplying fast, glycolytic
2 muscle fibers being preferentially recruited first.

3

4 *Intracellular Oxygenation*

5 An NIRS instrument (NIRO-300 + Detection Fiber Adapter Kit, Hamamatsu
6 Photonics, Shizuoka, Japan) was used to measure the oxygenation of Mb. The distance
7 between the photodiode and the LED was fixed at 10 mm. The toe of the foot was secured by
8 a clamp with the rat laid on its back. After that, the NIRS probes were firmly attached to the
9 skin of the gastrocnemius muscle and were fixed by clamps on both sides of the muscle.
10 During the initial period, for at least 30 sec before the start of contraction, the average
11 fluctuation in the NIRS signals was adjusted to a reference value of zero. After the exercise
12 protocol, the anoxic buffer, equilibrated with 95%N₂ + 5%CO₂ gas was perfused for 30 min to
13 obtain the maximal Mb desaturation value. The equilibrium period with the anoxic buffer was
14 initiated after a 5 min recovery and after the NIRS signals had returned to baseline level. After
15 30 min, the NIRS signal reached a steady state. The muscle then received electrical
16 stimulation to contract for 2 min. No further increase in Δ [deoxy-Mb] signal was evident. The
17 final Δ [deoxy-Mb] signal intensity served as the normalization constant for 100% Mb
18 deoxygenation.

19

20 *Data acquisition*

21 The sampling rate for the NIRS data was 1 Hz. The other parameters (tension,
22 perfusion pressure, O₂ content at the inflow and outflow) were collected using a data
23 acquisition system (PowerLab 8SP, AD Instruments, Australia) at a sampling rate of 1 kHz.
24 All the data were transferred to a personal computer with acquisition software (Chart ver.
25 5.5.6. AD Instruments)

1 *Data Analysis*

2 A simple moving average smoothed the $\Delta[\text{deoxy-Mb}]$ and the $\Delta[\text{oxy-Mb}]$ NIRS
3 signal using a rolling average of 5 points, which correspond to a time frame of 5 sec (Box *et*
4 *al.* 1978). The $\Delta[\text{deoxy-Mb}]$ kinetics were calibrated against two different values of the NIRS
5 signal: one at rest and the other during steady state with anoxia buffer perfusion. These values
6 correspond to the initial Mb desaturation of 10% and the final Mb desaturation of 100%,
7 respectively. While the S_{mbO_2} at rest could not be determined by NIRS, the value was
8 assumed to be 90% based on the previous studies that reported the S_{mbO_2} at rest was greater
9 than 90% (Chung *et al.* 2005; Richardson *et al.* 2006).

10 The $\% \Delta[\text{deoxy-Mb}]$ plots were converted to S_{mbO_2} plots using the following
11 equation;

12

$$13 \quad S_{\text{mbO}_2} (\%) = 100 - \% \Delta[\text{deoxy-Mb}]$$

14

15 The S_{mbO_2} kinetics shows no evidence for any slow component of Mb desaturation. Therefore,
16 the S_{mbO_2} plots were fitted by the following single exponential equation to calculate the
17 kinetics parameters using an iterative least-squares technique by means of a commercial
18 graphing/analysis package (KaleidaGraph 3.6.1).

19

$$20 \quad S_{\text{mbO}_2} (\%) = \text{BL} + \text{AP} [1 - \exp^{-(t - \text{TD})/\tau}]$$

21

22 The parameter values, where BL was the baseline value, AP was the amplitude
23 between BL and the steady-state value during the exponential component, TD was the time
24 delay between the start of contraction and the appearance of the S_{mbO_2} signals, and τ was the
25 time constant of the kinetics of the S_{mbO_2} signal. The S_{mbO_2} kinetics were modeled as an

1 exponential function. Since $\dot{m}\dot{V}O_2$ increases rapidly without any time delay, the mean
2 response time (MRT) calculated by $TD + \tau$ was used as an effective parameter of the response
3 time for Mb deoxygenation at the onset of muscle contraction (Behnke *et al.* 2002; Rossiter *et*
4 *al.* 1999). Moreover, MRT indicates the time to require to reach 63% of AP. Dividing 63% of
5 AP by MRT gives a value for the time-dependent change in Mb deoxygenation. The
6 parameter $_{0.63}AP/MRT$ for $S_{mb}O_2$ shows the Mb O_2 release rate, which indicates the amount of
7 oxygen released by Mb per unit time at the onset of exercise. The Mb O_2 release rate was
8 calculated by using the following equation:

9

$$10 \quad Mb \text{ O}_2 \text{ release rate} = (_{0.63}AP / MRT) [Mb]$$

11

12 where the $_{0.63}AP/MRT$ for $S_{mb}O_2$ was Mb deoxygenation rate in %/sec, and [Mb] in the
13 hindquarter was $0.119 \pm 0.023 \mu\text{mol/g}$ tissue. Inserting this value for Mb into the equation led
14 to the determination of the Mb O_2 release rate in $\mu\text{mol/g/min}$.

15 Based on the result of the $S_{mb}O_2$ kinetics parameters, the model $S_{mb}O_2$ kinetics was
16 re-constructed. The model $S_{mb}O_2$ kinetics was converted to $P_{mb}O_2$ using the following
17 equation;

18

$$19 \quad P_{mb}O_2 \text{ (mmHg)} = (S_{mb}O_2 / (1 - S_{mb}O_2)) P_{50}$$

20

21 where P_{50} is the partial oxygen pressure required to half-saturate Mb and a P_{50} of 2.4 mmHg
22 was used for the equation, assuming a muscle temperature of 37 °C (Schenkman *et al.* 1997).
23 The calculated $P_{mb}O_2$ plots were mathematically evaluated to get the MRT of its kinetics by
24 using the same single exponential equation as for $S_{mb}O_2$. The $_{0.63}AP/MRT$ for $P_{mb}O_2$ indicates
25 decremental rate of $P_{mb}O_2$ at the onset of muscle contraction. The $P_{mb}O_2$ at the steady state

1 was calculated by directly using the value for $S_{mb}O_2$ at the steady state. Moreover, since the
2 partial pressure of O_2 corresponds to a specific amount of dissolved O_2 in solution,
3 intracellular $[O_2]$ was calculated from $P_{mb}O_2$ value at rest and at each exercise intensity using
4 the following equation.

5

$$6 \quad \text{Intracellular } [O_2] \text{ (}\mu\text{M)} = P_{mb}O_2 \times O_2 \text{ solubility}$$

7

8 where $P_{mb}O_2$ is in mmHg, and the solubility of O_2 in buffer is $0.00135 \mu\text{mol/ml/mmHg}$ at 37
9 $^\circ\text{C}$ (Philip and Dorothy, 1971).

10

11 *Muscle oxygen consumption*

12 $m\dot{V}O_2$ was calculated from the arteriovenous oxygen content difference multiplied
13 by the flow rate, using the equation:

14

$$15 \quad m\dot{V}O_2 \text{ (}\mu\text{mol/g/min)} = \text{flow rate} \times ((PO_{2in} - PO_{2out}) \times O_2 \text{ solubility}) / \text{muscle weight}$$

16

17 where flow rate is the flow in ml/min, and PO_{2in} and PO_{2out} are the arterial and venous
18 oxygen tensions after adjusting for the vapor pressure of water. Inflow PO_2 and outflow PO_2
19 were measured continuously using two O_2 electrodes (5300A, YSI, USA) along tubing before
20 and after perfusing to the hindlimb. The vapor pressure at 37°C is 47.03 mmHg . The
21 solubility of oxygen in the buffer is $0.00135 \mu\text{mol per ml per mmHg}$ at 37°C (Philip and
22 Dorothy 1971). The $m\dot{V}O_2$ at rest and during muscle contraction was calculated by using the
23 values of $PO_{2in} - PO_{2out}$ averaged over 15 sec at the steady state condition before and during
24 muscle contraction. Also, the average rate increase in $m\dot{V}O_2$ was calculated by dividing
25 $m\dot{V}O_2$ by 2 min, the period of muscle contraction, because the response time of the O_2

1 electrodes was too slow to follow the on-kinetics of $m\dot{V}O_2$.

2

3 *Tissue Preparation and Optical Measurement*

4 After the buffer perfusion, the hindlimb muscles were isolated and immediately
5 weighed, thoroughly minced using stainless steel scissors, and homogenized in an ice bath
6 with phosphate buffer (0.04 M, pH 6.6) bubbled with carbon monoxide (CO). The
7 homogenate was then separated by centrifugation at 12,000 g for 30 min at 4 °C. The clear
8 supernatant was decanted into a small glass tube and again equilibrated with CO to ensure
9 binding to Mb. The optical density at 538 nm (β band) and 568 nm (α band) was used for
10 calculation of both the Hb and Mb concentration in the muscle tissue as described in a
11 modified Reynafarje method (Masuda *et al.* 2008).

12

13 *Statistical Analyses*

14 All data are expressed as the mean \pm SD. Differences between tension levels were
15 examined using repeated measures ANOVA. The Tukey-Kramer's post-hoc test was applied if
16 ANOVA indicated a significant difference. Pearson's correlation coefficient was calculated
17 when the relationship between two variables was evaluated. The level of significance was set
18 at $p < 0.05$.

19

20

21 **Results**

22

23 Figure 1 shows a wave pattern of a single contraction and the time-course change of
24 the twitch tension at each exercise intensity. An isometric twitch contraction was evoked by
25 stimulating the sciatic nerve electrically. The stimulation consisted of a single square wave

1 (delay: 10 μ sec, duration: 1 msec) controlled by an electro stimulator system. Twitch
2 contractions typically show a staircase effect. Twitch contraction showed staircase effect of
3 $17.2 \pm 4.2\%$, $21.8 \pm 5.7\%$, and $20.9 \pm 12.0\%$ at 50, 75 and 100% of maximal contraction,
4 which lasted for a total of 120 sec. However, these staircase effects do not affect the Mb
5 desaturation rate, which shows no evidence of a slow component. The muscle also shows no
6 sign of fatigue, even during the highest stimulation intensity.

7 Table 1 summarizes twitch tensions, $m\dot{V}O_2$, rate increase in $m\dot{V}O_2$ and O_2 release
8 rate of Mb during contractions at different intensities. As the muscle tension increased
9 significantly from 382 mN to 738 mN, the $m\dot{V}O_2$ also increased from 0.46 μ mol/g/min at rest
10 to 0.56-0.69 μ mol/g/min during muscle contraction. Moreover, rate increase in $m\dot{V}O_2$ and Mb
11 O_2 release rate significantly increase with the tension level. The lactate to pyruvate ratio (L/P)
12 remains constant and shows no significant increase from the resting muscle value
13 (Bylund-Fellenius *et al.* 1981). If oxygen availability were limiting, lactate level should rise,
14 as anaerobic glycolysis starts. Indeed, the L/P increases during perfusion with anoxia buffer
15 (95% N_2) increases. O_2 availability and delivery can sustain maximal contraction with no sign
16 of fatigue.

17 Figure 2 shows representative Δ [deoxy-Mb] and Δ [oxy-Mb] kinetics during different
18 levels of twitch contractions and under anoxic-perfusion as assessed by NIRS. The Roman
19 numerals I, II and III represent the NIRS signal response to 1 Hz twitch contractions at 50%,
20 75% and 100% of maximal twitch tension. In protocol IV, the non-contracting muscle
21 received a perfusated 95% N_2 + 5% CO_2 .

22 The Δ [deoxy-Mb] and Δ [oxy-Mb] signals increased and decreased at the onset of
23 contraction, respectively. The AP of Δ [deoxy-Mb] kinetics increases to 4-15 μ mol \cdot cm as
24 muscle tension rises (states I-III). The Δ [deoxy-Mb] and Δ [oxy-Mb] signal under perfusion
25 with 95% N_2 + 5% CO_2 rose and declined further than the signal observed during protocols

1 I-III. The NIRS signals reached a steady state within 10 min. The steady state value of
2 $\Delta[\text{deoxy-Mb}]$ obtained under anoxic-perfusion was assumed to represent fully desaturated Mb
3 ($S_{\text{mbO}_2} = 0\%$). Mb saturation during the resting condition was assumed to be 90% saturated.

4 Figure 3 shows the kinetics of S_{mbO_2} and P_{mbO_2} during maximal twitch contraction.
5 The plot fits the representative data from a single experiment using protocol III. The
6 $\Delta[\text{deoxy-Mb}]$ was used to calculate the S_{mbO_2} , which (A) declines with an MRT of 45 sec.
7 The corresponding P_{mbO_2} curve (B), converted from S_{mbO_2} , shows a faster, steeper decline
8 than the S_{mbO_2} curve and exhibits a shorter MRT of 28 sec. At the maximal twitch tension,
9 S_{mbO_2} and P_{mbO_2} reached the respective values of 49% and 2.4 mmHg .

10 Table 3 summarizes the kinetic parameters for S_{mbO_2} and P_{mbO_2} during different
11 intensities of twitch contraction. The S_{mbO_2} and P_{mbO_2} during exercise decreased, and the
12 MRT for S_{mbO_2} and P_{mbO_2} kinetics also decreased as work intensity rose ($p < 0.05$).

13 Figure 4 shows the relationship between S_{mbO_2} and relative work intensity. The work
14 intensity was normalized by maximal twitch tension in each animal. S_{mbO_2} decreased
15 significantly as work intensity increased. The steady state level of S_{mbO_2} declined from 90%
16 at rest to $70.7 \pm 7.1\%$, $59.2 \pm 7.4\%$ and $49.3 \pm 7.3\%$ at 50%, 75% and 100% of maximal
17 contraction, respectively.

18 Figure 5 shows the relationship between intracellular $[\text{O}_2]$ and $\Delta m\dot{V}\text{O}_2$ during twitch
19 contraction. The intracellular $[\text{O}_2]$ was based on the Mb equilibrium with P_{mbO_2} . The
20 intracellular $[\text{O}_2]$ decreased sharply from 29.2 μM at rest to $8.5 \pm 3.4 \mu\text{M}$, $5.0 \pm 1.8 \mu\text{M}$ and
21 $3.3 \pm 1.0 \mu\text{M}$ at each increased work level, while the value of intracellular $[\text{O}_2]$ decreased
22 exponentially with $\Delta m\dot{V}\text{O}_2$.

23 Figure 6 shows the relationship between Mb O_2 release rate at the onset of
24 contraction and $\Delta m\dot{V}\text{O}_2$. The Mb O_2 release rate (1.4 ± 0.5 , 2.8 ± 0.5 , and $4.2 \pm 0.7 \cdot 10^{-2}$
25 $\mu\text{mol/g/min}$) increased progressively with contraction force and $\Delta m\dot{V}\text{O}_2$.

1 **Discussion**

2

3 *Intracellular $S_{mb}O_2$ and $P_{mb}O_2$ during muscle contraction*

4 At the onset of muscle contraction, Mb desaturates immediately and rapidly in an
5 exponential manner and reaches a steady state level, which depends upon the work intensity.
6 As the work intensity and $m\dot{V}O_2$ increase, the steady-state level of $S_{mb}O_2$ falls from 90% at
7 rest to 71%, 59%, and 49% at 50%, 75%, and 100% of maximal contraction. The progressive
8 Mb desaturation with increased work agrees with the 1H -MRS observation in contracting
9 human leg muscle (Molé *et al.* 1999). $P_{mb}O_2$ during contraction decreases correspondingly
10 from 6.3 to 2.4 mmHg.

11 Even as O_2 tension falls during muscle contraction, it never reaches a critical $P_{mb}O_2$
12 to limit respiration or oxidative phosphorylation (Kreutzer *et al.* 1992) or $m\dot{V}O_2$ (Table 1).
13 Under all contraction conditions, the L/P remains constant and shows no presence of
14 hypoxemia or ischemia.

15 In fact, as PO_2 falls with work intensity, $m\dot{V}O_2$ rises. From an enzyme kinetics
16 vantage, the rising $m\dot{V}O_2$ with increased contraction intensity in the face of a declining PO_2
17 raises questions about O_2 as the limiting substrate in regulating the cytochrome reaction rate.
18 If the O_2 supply alone regulates the respiration, then the rising $m\dot{V}O_2$ requires an increased O_2
19 supply instead of the observed decrease (Chung *et al.* 2005; Jue 2004).

20

21 *O_2 Gradient*

22 As muscle contraction begins, the $P_{mb}O_2$ decreases immediately to expand the O_2
23 gradient ($\Delta PO_2/\mu m$) from the capillary to the cell in order to meet the increased energy
24 demand, as expressed in the following equation:

25

1
$$m\dot{V}O_2 = k DO_2 (P_{cap}O_2 - P_{mb}O_2)$$

2

3 where DO_2 is the O_2 diffusion conductance and $P_{cap}O_2$ is the PO_2 in the capillary. In the
4 constant-flow hindlimb model, DO_2 does not contribute significantly, since a 30-min
5 equilibrium period elicited a flow-induced vasodilatation. The perfusive O_2 conductance
6 remains constant (Hepple *et al.* 2003).

7 As $m\dot{V}O_2$ rises with muscle contraction, $P_{cap}O_2$ and/or $P_{mb}O_2$ must then change to
8 enhance the O_2 flux into the cell. However, studies have shown that $P_{cap}O_2$ actually decreases
9 from 31.4 (at rest) to 21.0 mmHg during 1 Hz maximal twitch contractions ($\Delta 10.4$ mmHg,
10 Behnke *et al.* 2001). If the O_2 gradient has any significant role, then the $\Delta P_{mb}O_2$ must decline
11 even further. Indeed, the $\Delta P_{mb}O_2$ exceeds the $\Delta P_{cap}O_2$ ($\Delta 19.2$ mmHg vs. $\Delta 10.4$ mmHg). The
12 increase in $m\dot{V}O_2$ during muscle contraction depends then on the expansion of O_2 gradient as
13 shown in Table 4.

14 Such an expansion of the O_2 gradient does not appear localized only to the buffer
15 perfused hindlimb model, because buffer carries less O_2 than blood. In contracting human
16 skeletal muscle, all 1H -MRS data show Mb desaturation, consistent with a decreased
17 intracellular $P_{mb}O_2$ (Molé *et al.* 1999; Richardson *et al.* 1995). Furthermore, Molé *et al.*
18 (1999) has indicated that the $P_{mb}O_2$ drops progressively and reaches 3.1 mmHg at peak
19 gastrocnemius muscle contraction.

20

21 *Change in the Kinetics of $S_{mb}O_2$ and Mb O_2 release rate with Oxygen Demand*

22 The $P_{cap}O_2$, however, does not start to change until about 20 sec, after the onset of
23 muscle contraction. Yet $m\dot{V}O_2$ has already increased. Some researchers have postulated that
24 during this initial period, capillary to cell distance must adjust to increase the DO_2 , which
25 increases the O_2 flux to match the rising $m\dot{V}O_2$ (Behnke *et al.* 2001). These researchers have

1 assumed the O₂ gradient does not play a significant role. However, the present study shows a
2 rapid drop in intracellular P_{mb}O₂ and indicates that the O₂ gradient widens quickly.

3 Even as the O₂ gradient widens and m $\dot{V}O_2$ rises immediately, vascular O₂ flux still
4 does not provide a significant amount of the initial O₂, since P_{cap}O₂ appears constant for about
5 20 sec. Instead, the initial O₂ comes in part from Mb, as evidenced by the rapid fall in S_{mb}O₂.
6 Mb releases its O₂ at rate of 1.4 ± 0.5 to 2.8 ± 0.5 and 4.2 ± 0.7 10⁻² μmol/g/min as the work
7 intensity increases. Even though Mb supplies the primary source of O₂ at the onset of
8 contraction, it provides only about 30% of the average rate of increase in m $\dot{V}O_2$ from 5.3 ±
9 1.8 to 7.8 ± 1.5 to 10.9 ± 3.4 10⁻² μmol/g/min². However, because of insufficient response time
10 of the O₂ electrodes to allow analysis of m $\dot{V}O_2$ on-kinetics, the limited time resolution of the
11 m $\dot{V}O_2$ precludes currently an accurate assessment of the O₂ contribution of Mb at the onset of
12 contraction. It may provide all the O₂ at the start of contraction. Such a view implies at least a
13 biphasic increase in m $\dot{V}O_2$, consistent with previous reports (Molé *et al.* 1999; Whipp *et al.*
14 1999).

15 Contracting human leg muscle also shows Mb desaturates with a time constant of
16 about 25 sec. Indeed, investigators have interpreted the Mb desaturation kinetics as an index
17 of intracellular m $\dot{V}O_2$ and have suggested a mechanism underlying the biphasic increase in
18 m $\dot{V}O_2$ as muscle contraction commences (Chung *et al.* 2005).

19

20 *Mb as an O₂ buffer*

21 MRT of P_{mb}O₂ provides insight into role of Mb as an immediate O₂ source. The
22 investigation using isolated myoglobin-free myocytes from *Xenopus laevis* showed 35.2 ± 5.1
23 sec in MRT for ~20 mmHg of net depression in intracellular PO₂ during tetanic contractions
24 (Kindig *et al.* 2003). The present study observes an MRT of 27.7 ± 3.1 sec. The slower MRT
25 in *Xenopus laevis* myocyte may arise from the lack of Mb facilitated O₂ transport, and

1 therefore contracting myocytes require a significantly greater extracellular PO_2 to achieve a
2 given $m\dot{V}O_2$ (Hogan *et al.* 2001; Kindig *et al.* 2003). The present study suggests that Mb
3 provides an immediate O_2 source for the sudden rise in mitochondrial respiration.

4 Both the perfused hindlimb and human leg experiments point to a similar conclusion:
5 at the start of contraction, a sudden mismatch of O_2 supply and demand appears. Mb buffers
6 the sudden increase in O_2 demand as respiration rises rapidly (Molé *et al.* 1999; Chung *et al.*
7 2005).

8 9 *The relationship between $P_{mb}O_2$ kinetics and muscle oxygen consumption*

10 At the highest muscle contraction intensity employed in the present study $P_{mb}O_2$
11 began to decrease with an MRT of 25 sec while the MRT of $P_{cap}O_2$ was 40.9 sec at 1 Hz
12 muscle contraction (Behnke *et al.* 2001). Therefore, the MRT of $P_{mb}O_2$ is shorter than that for
13 $P_{cap}O_2$ at maximal muscle contraction. This difference suggests that the presence of Mb
14 allows the intracellular O_2 environment to adjust more effectively to the abrupt increase in
15 oxygen demand at the onset of muscle contraction, before the microcirculatory O_2
16 environment adapts. Mitochondrial respiration accelerates without a discernible delay after
17 the onset of the muscle contraction (Balaban *et al.* 2003). In fact, $m\dot{V}O_2$ begins to increase
18 without a time delay during muscle contraction (Behnke *et al.* 2002). The 23 sec MRT of
19 $m\dot{V}O_2$ is consistent with the 25 sec MRT for $P_{mb}O_2$ observed in human leg studies (Behnke *et*
20 *al.* 2002; Chung *et al.* 2005).

21 22 *Limitations of the NIRS perfusion model for the determination of PO_2*

23 Some studies have pointed out the importance of surprisingly large extracellular PO_2
24 gradients (Gnaiger *et al.* 1995). However, intracellular PO_2 gradients may also increase at
25 increased O_2 flux, so that they affect mitochondrial respiration as a consequence of decreased

1 cytoplasmic O₂ concentration surrounding mitochondria in the “anoxic core” (Takahashi *et al.*
2 1998, 1999). Taken together, significant gradients of Mb oxygenation could be produced in
3 the cytoplasm of the *in vivo* heart (Takahashi *et al.* 2000). On the other hand, in the classical
4 view, Mb facilitates O₂ transport within exercising myocytes (Wittenberg and Wittenberg
5 1989) and that produces relatively homogeneous cytoplasmic PO₂ distribution even during
6 maximal aerobic work (Honig *et al.* 1997; Jones 1986). Mb translational diffusion in the cell,
7 however, appears too slow to have a significant transport role in the steady state
8 (Papadopoulos *et al.* 2001; Lin *et al.* 2007b). However, it may still play a significant role in
9 the transient state, when the PO₂ falls precipitously (Lin *et al.* 2007a). Unfortunately, the
10 NIRS measurements cannot shed insight into these issues. The P_{mb}O₂ gradient and Mb
11 facilitated O₂ diffusion within the cell remain controversial.

12 The previous ¹H-MRS study did not detect the proximal histidyl N₈H F8 of
13 deoxy-Mb under resting conditions, even though this experimental technique can
14 quantitatively detect the deoxy-Mb signal at ~10% deoxygenation in these calf experiments
15 (Chung *et al.* 2005). Given the *in vitro* Mb P₅₀ of 2.4 mmHg at 37 °C, the fact that the
16 deoxy-Mb signal could not be detected in the resting state implies that the P_{mb}O₂ must
17 saturate >90% of the Mb, or that P_{mb}O₂ is > 21.6 mmHg (Chung *et al.* 2005). Another study
18 reported the Mb saturation level as 91 ± 1% in normoxia at rest (Richardson *et al.* 2006). In
19 contrast, Schenkman *et al.* (2001) reported that the average baseline Mb saturation during
20 perfusion with a 95% O₂ + 5% CO₂ equilibrated buffer was 72% at rest. Thus, the resting value
21 of S_{mb}O₂ remains controversial. However, under nitrogen-equilibrated buffer perfusion, the
22 Δ[deoxy-Mb] signal no longer increases even following evoked muscle contraction. Mb is
23 likely to be full deoxygenated under such conditions.

24

25

1 *Conclusions*

2 The present study has used NIRS to determine the intracellular O₂ dynamics and
3 has observed that Mb desaturates progressively with an increase in oxygen demand, reflecting
4 a progressive decrease in intracellular PO₂. The immediate decrease in P_{mb}O₂ leads to an
5 expansion of the O₂ gradient, which enhances the O₂ flux to meet the increased $\dot{m}\dot{V}O_2$.
6 Moreover, the O₂ released from Mb likely supply the initial O₂ for respiration.

1 **Acknowledgements**

2

3 This research was supported by a Grant-in-Aid for Scientific Research from the
4 Japanese Ministry of Education, Science, Sports and Culture (20680032, 21650167, KM), and
5 partial support from the Yamaha Motor Foundation for Sports (KM) and the Nakatomi
6 Foundation (KM).

7

1 **References**

2 Balaban RS, Bose S, French SA & Territo PR (2003). Role of calcium in metabolic signaling
3 between cardiac sarcoplasmic reticulum and mitochondria *in vitro*. *Am J Physiol Cell Physiol*
4 **284**, C285-C293.

5
6 Behnke BJ, Barstow TJ, Kindig CA, McDonough P, Musch TI & Poole DC (2002). Dynamics
7 of oxygen uptake following exercise onset in rat skeletal muscle. *Respir Physiol Neurobiol*
8 **133**, 229-239.

9
10 Behnke BJ, Kindig CA, Musch TI, Koga S & Poole DC (2001). Dynamics of microvascular
11 oxygen pressure across the rest-exercise transition in rat skeletal muscle. *Respir Physiol* **126**,
12 53-63.

13
14 Box GEP, Hunter WG & Hunter JS (1978). Statistics for experimenters: An introduction to
15 design, data analysis, and model building. New York: John Wiley & Sons.

16
17 Bylund-Fellenius AC, Walker PM, Elander A, Holm S, Holm J & Scherstén T (1981). Energy
18 metabolism in relation to oxygen partial pressure in human skeletal muscle during exercise.
19 *Biochem J* **200**, 247-255.

20
21 Chung YR, Molé PA, Sailasuta N, Tran TK, Hurd R & Jue T (2005). Control of respiration
22 and bioenergetics during muscle contraction. *Am J Physiol Cell Physiol* **288**, C730-C738.

23
24 Gnaiger E, Steinlechner-Maran R, Méndez G, Eberl T & Margreiter R (1995). Control of
25 mitochondrial and cellular respiration by oxygen. *J Bioenerg Biomembr* **27**, 583-596.

26
27 Hepple RT, Krause DJ, Hagen JL & Jackson CC (2003). $\dot{V}O_2$ max is unaffected by altering
28 the temporal pattern of stimulation frequency in rat hindlimb *in situ*. *J Appl Physiol* **95**,
29 705-711.

30
31 Honig CR, Gayeski TEJ & Groebe K (1997). Myoglobin and oxygen gradients. In *The Lung:*
32 *Scientific Foundations*, pp. 1925-1933. Raven, Philadelphia.

33
34 Hogan MC (2001). Fall in intracellular PO_2 at the onset of contractions in *Xenopus* single
35 skeletal muscle fibers. *J Appl Physiol* **90**, 1871-1876.

36
37 Jones DP (1986). Intracellular diffusion gradients of O_2 and ATP. *Am J Physiol Cell Physiol*
38 **250**, C663-C675.

39
40 Jue T (2004). Bioenergetics implication of metabolic fluctuation during muscle contraction.
41 In *Metabolomics by in vivo NMR*, ed. Shulman RG & Rothman DL, pp. 104-117. John Wiley,
42 Chichester.

43
44 Kindig CA, Howlett RA & Hogan MC (2003). Effect of extracellular PO_2 on the fall in
45 intracellular PO_2 in contracting single myocytes. *J Appl Physiol* **94**, 1964-1970.

46
47 Kreutzer U, Wang DS & Jue T (1992). Observing the 1H NMR signal of the myoglobin
48 Val-E11 in myocardium: an index of cellular oxygenation. *Proc Natl Acad Sci USA* **89**,

- 1 4731-4733.
2
- 3 Lin PC, Kreutzer U & Jue T (2007a). Anisotropy and temperature dependence of myoglobin
4 translational diffusion in myocardium: implication for oxygen transport and cellular
5 architecture. *Biophys J* **92**, 2608-2620.
6
- 7 Lin PC, Kreutzer U & Jue T (2007b). Myoglobin translational diffusion in rat myocardium
8 and its implication on intracellular oxygen transport. *J Physiol* **578**, 595-603.
9
- 10 Masuda K, Takakura H, Furuichi Y, Iwase S & Jue T (2010). NIRS measurement of O₂
11 dynamics in contracting blood and buffer perfused hindlimb muscle. *Adv Exp Med Biol* **662**,
12 323-328.
13
- 14 Masuda K, Truscott K, Lin PC, Kreutzer U, Chung YR, Sriram R & Jue T (2008).
15 Determination of myoglobin concentration in blood-perfused tissue. *Eur J Appl Physiol* **104**,
16 41-48.
17
- 18 McDonough P, Behnke BJ, Padilla DJ, Musch TI & Poole DC (2005). Control of
19 microvascular oxygen pressures in rat muscles comprised of different fibre types. *J Physiol*
20 **563**, 903-913.
21
- 22 Molé PA, Chung YR, Tran TK, Sailasuta N, Hurd R & Jue T (1999). Myoglobin desaturation
23 with exercise intensity in human gastrocnemius muscle. *Am J Physiol Regul Integr Comp*
24 *Physiol* **277**, R173-R180.
25
- 26 Papadopoulos S, Endeward V, Revesz-Walker B, Jurgens KD & Gros G (2001). Radial and
27 longitudinal diffusion of myoglobin in single living heart and skeletal muscle cells. *Proc Natl*
28 *Acad Sci USA* **98**, 5904-5909.
29
- 30 Philip LA & Dorothy SD (1971). *Respiration and Circulation*. Fed of Am Societies for
31 Experimental Biology, Bethesda.
32
- 33 Poole DC, Ferreira LF, Behnke BJ, Barstow TJ & Jones AM (2007). The final frontier:
34 oxygen flux into muscle at exercise onset. *Exerc Sport Sci Rev* **35**, 166-173.
35
- 36 Richardson RS, Duteil S, Wary C, Wray DW, Hoff J & Carlier PG (2006). Human skeletal
37 muscle intracellular oxygenation: the impact of ambient oxygen availability. *J Physiol* **571**,
38 415-424.
39
- 40 Richardson RS, Noyszewski EA, Kendrick KF, Leigh JS & Wagner PD (1995). Myoglobin O₂
41 Desaturation During Exercise - Evidence of Limited O₂ Transport. *J Clin Invest* **96**,
42 1916-1926.
43
- 44 Rossiter HB, Ward SA, Doyle VL, Howe FA, Griffiths JR & Whipp BJ (1999). Inferences
45 from pulmonary O₂ uptake with respect to intramuscular [phosphocreatine] kinetics during
46 moderate exercise in humans. *J Physiol* **518**, 921-932.
47
- 48 Schenkman KA (2001). Cardiac performance as a function of intracellular oxygen tension in
49 buffer-perfused hearts. *Am J Physiol Heart Circ Physiol* **281**, H2463-H2472.

- 1
2 Schenkman KA, Marble DR, Burns DH & Feigl EO (1997). Myoglobin oxygen dissociation
3 by multiwavelength spectroscopy. *J Appl Physiol* **82**, 86-92.
4
5 Shiota M & Sugano T (1986). Characteristics of rat hindlimbs perfused with erythrocyte- and
6 albumin-free medium. *Am J Physiol* **251**, C78-C84.
7
8 Takahashi E, Endoh H & Doi K (1999). Intracellular gradients of O₂ supply to mitochondria
9 in actively respiring single cardiomyocyte of rats. *Am J Physiol* **276**, H718-H724.
10
11 Takahashi E, Endoh H & Doi K (2000). Visualization of myoglobin-facilitated mitochondrial
12 O₂ delivery in a single isolated cardiomyocyte. *Biophys J* **78**, 3252-3259.
13
14 Takahashi E, Sato K, Endoh H, Xu ZL & Doi K (1998). Direct observation of radial
15 intracellular PO₂ gradients in a single cardiomyocyte of the rat. *Am J Physiol* **275**,
16 H225-H233.
17
18 Whipp BJ, Rossiter HB, Ward SA, Avery D, Doyle VL, Howe FA & Griffiths JR (1999).
19 Simultaneous determination of muscle ³¹P and O₂ uptake kinetics during whole body NMR
20 spectroscopy. *J Appl Physiol* **86**, 742-747.
21
22 Wittenberg BA & Wittenberg JB (1989). Transport of oxygen in muscle. *Annu Rev Physiol* **51**,
23 857-878.
24

1 **Figure Legends**

2

3 **Figure 1.**

4 **Representative muscle tension generation during muscle contraction for 120 sec from a**
5 **single experiment.**

6 Twitch muscle contractions were elicited every 1 sec (1 Hz). The target tension levels were
7 set at 50%, 75% and 100% twitch tension under buffer-perfused condition, and were
8 controlled by changing the voltage of the stimuli (3-8 volts). In this figure, a wave pattern of a
9 single contraction and the time-course change of the twitch tension at the each exercise
10 intensity were shown. No sign of fatigue was observed during muscle contraction regardless
11 of the exercise intensity.

12

13 **Figure 2.**

14 **Representative time course of the Δ [deoxy-Mb] and Δ [oxy-Mb] NIRS signals during**
15 **different levels of twitch contractions (I-III) and under anoxic-perfusion (IV).**

16 The arrows indicate the onset of contraction (I-III) and anoxic-perfusion (95%N₂ + 5%CO₂)
17 (IV). Protocols I, II and III use 1 Hz stimulation to reach 50%, 75%, and 100% of maximal
18 twitch tension The Δ [deoxy-Mb] and Δ [oxy-Mb] signals change immediately at the onset of
19 contraction, and reach an Δ [deoxy-Mb] AP values of 4-15 $\mu\text{mol} \cdot \text{cm}$ (I-III). Under anoxia
20 buffer perfusion condition, the Δ [deoxy-Mb] signal rises to higher AP value within 10 min.

21

22 **Figure 3.**

23 **Representative kinetics of Mb saturation ($S_{\text{mb}}\text{O}_2$) and intracellular oxygen tension**
24 **($P_{\text{mb}}\text{O}_2$) during maximal twitch contraction (1 Hz).**

25 The calculated $S_{\text{mb}}\text{O}_2$ (A) declines with an MRT of 44 sec. The $P_{\text{mb}}\text{O}_2$ (B), converted from the

1 $S_{mb}O_2$, using a P_{50} at 37 °C of 2.4 mmHg shows a faster and steeper decline than the $S_{mb}O_2$
2 curve (Schenkman *et al.* 1997). It has an MRT of 28 sec. At the maximal twitch tension,
3 $S_{mb}O_2$ and $P_{mb}O_2$ reached 49% and 2.4 mmHg, respectively.

4
5 **Figure 4.**

6 **Relationship between the Mb saturation ($S_{mb}O_2$) and work intensity during twitch**
7 **contraction.**

8 The $S_{mb}O_2$ during twitch contraction decreases linearly as a function of work intensity. The
9 work intensity was normalized by maximal twitch tension in each animal. The regression line
10 is based on mean values ($S_{mb}O_2 = 93.95 - 0.45 \cdot \text{work intensity}$, $r = -0.81$, $p < 0.01$, $n = 6$).

11 Each data point represents the mean \pm SD.

12
13 **Figure 5.**

14 **Relationship between intracellular $[O_2]$ and muscle oxygen consumption ($\Delta m\dot{V}O_2$)**
15 **during twitch contraction.**

16 Intracellular $[O_2]$ (μM) decreased from 29.2 at rest to 8.5 ± 3.4 , 5.0 ± 1.8 and 3.3 ± 1.0 at each
17 tension level, and continues to gradually decrease as oxygen is consumed ($\Delta m\dot{V}O_2$)

18 ($\text{Intracellular } [O_2] = 29.2 - 27.8 \cdot (1 - \exp^{-0.08 \Delta m\dot{V}O_2})$, $r = 0.99$). The $m\dot{V}O_2$ value represents the
19 average value of $m\dot{V}O_2$ for 15 sec at the steady state during muscle contraction. The data
20 point around the 30 μM of intracellular $[O_2]$ represents intracellular $[O_2]$ at rest of 29.2 μM .

21 The curvilinear line is based on mean values ($n = 6$). Each data point represents the mean \pm
22 SD.

23
24 **Figure 6.**

25 **Relationship between Mb O_2 release rate and muscle oxygen consumption ($\Delta m\dot{V}O_2$) at**

1 **the onset of contraction.**

2 Mb released O₂ immediately after the onset of contraction, and the resulting oxygen release

3 from Mb within myocyte increases with $\Delta m\dot{V}O_2$ (Mb O₂ release rate = 17.6 $\Delta m\dot{V}O_2$, r = 0.71,

4 p < 0.01). The regression line is based on mean values. Each data point represents the mean \pm

5 SD.

6

1
2
3
4
5
6**Table 1****Physiological parameters at the each exercise intensity**

Tension Level	50%	75%	100%
Muscle Tension (mN)	382.5 ± 61.7	567.0 ± 94.3 ^a	738.1 ± 122.9 ^{ab}
mVO ₂ at rest (μmol/g/min)	0.46 ± 0.11	0.47 ± 0.09	0.47 ± 0.11
mVO ₂ during contraction (μmol/g/min)	0.56 ± 0.10	0.63 ± 0.09	0.69 ± 0.12 ^a
ΔmVO ₂ (μmol/g/min)	0.10 ± 0.04	0.16 ± 0.03	0.22 ± 0.07 ^{ab}
Rate increase in mVO ₂ (10 ⁻² • μmol/g/min ²)	5.3 ± 1.8	7.8 ± 1.5	10.9 ± 3.4 ^{ab}
O ₂ release rate of Mb (10 ⁻² • μmol/g/min)	1.4 ± 0.5	2.8 ± 0.5 ^a	4.2 ± 0.7 ^{ab}

7
8
9
10
11
12
13
14

Values are mean ± SD (n = 6). ΔmVO₂ is net increase in mVO₂ due to muscle contraction. Rate increase in mVO₂ was calculated by dividing ΔmVO₂ by contraction time (2 min). The Mb O₂ release rate indicated the amount of [O₂] released from Mb per given time. All parameters except for resting mVO₂ increased as increase in tension level. The superscripts indicate significant difference (a; vs. 50%, b; vs. 75%, p < 0.05).

1
2
3
4
5
6

Table 2

Lactate to pyruvate ratio at rest and at the each tension level

Rest	Tension Level		
	50%	75%	100%
19.8 ± 3.0	23.4 ± 3.4	22.8 ± 3.9	23.1 ± 4.3

7
8
9

Values are mean ± SD (n = 6) obtained after 2 min of muscle contraction. There was no significant difference in L/P during rest and contraction.

1
2
3
4
5
6
7

Table 3

S_{mb}O₂ and P_{mb}O₂ kinetics parameters during muscle contraction and anoxia buffer perfusion

Parameter (Unit)	Tension Level			
	50%	50%	50%	
S _{mb} O ₂ kinetics	Steady state value (%)	70.7 ± 7.1	59.2 ± 7.4 ^a	49.3 ± 7.3 ^{ab}
	AP (%)	-19.2 ± 7.1	-30.8 ± 7.4 ^a	-40.7 ± 7.3 ^{ab}
	MRT (sec)	63.7 ± 16.0	49.0 ± 7.9	44.6 ± 8.0 ^a
	^{0.63} AP/MRT (%/sec)	-0.19 ± 0.06	-0.40 ± 0.07 ^a	-0.58 ± 0.10 ^{ab}
P _{mb} O ₂ kinetics	Steady state value (mmHg)	6.3 ± 2.5	3.7 ± 1.3 ^a	2.4 ± 0.7 ^a
	AP (mmHg)	-15.3 ± 2.5	-17.9 ± 1.3 ^a	-19.2 ± 0.8 ^a
	MRT (sec)	43.7 ± 4.2	34.5 ± 7.1 ^a	27.7 ± 3.1 ^{ab}
	^{0.63} AP/MRT (mmHg/sec)	-0.21 ± 0.03	-0.33 ± 0.06 ^a	-0.42 ± 0.04 ^{ab}

8
9
10
11

Values are mean ± SD (n = 6). The superscripts indicate significant difference (a; vs. 50%, b; vs. 75%, c; vs. 100%, p < 0.05).

1
2
3
4
5
6**Table 4****Estimation of $m\dot{V}O_2$ based on O_2 gradient between mean capillary PO_2 and intracellular PO_2 during rest and muscle contraction**

Parameter (Unit)	Rest	Tension Level			Ref.
		50%	75%	100%	
$m\dot{V}O_2$ ($\mu M/g/min$)	465.7 ± 100.3	562.6 ± 96.7^d	626.2 ± 85.0^d	688.5 ± 120.1^{ad}	This paper
$\Delta m\dot{V}O_2$ ($\mu M/g/min$)	–	105.3 ± 36.2	156.0 ± 30.2	218.7 ± 67.2^{ab}	This paper
Microvascular PO_2 (mmHg)	31.4	(21.0)	(21.0)	21.0	Behnke <i>et al.</i> (2001)
Microvascular $[O_2]$ (μM)	42.4	(28.4)	(28.4)	28.4	Behnke <i>et al.</i> (2001)
Intracellular PO_2 (mmHg)	21.6 ± 0.0	6.3 ± 2.5^d	3.7 ± 1.3^{ad}	2.4 ± 0.7^{ad}	This paper
Intracellular $[O_2]$ (μM)	29.2 ± 0.0	8.5 ± 3.4^d	5.0 ± 1.8^{ad}	3.3 ± 1.0^{ad}	This paper
O_2 gradient (mmHg)	9.8 ± 0.0	14.7 ± 2.4^d	17.3 ± 1.3^{ad}	18.6 ± 0.7^{ad}	
O_2 gradient (μM)	13.2 ± 0.0	19.9 ± 3.4^d	23.4 ± 1.8^{ad}	25.0 ± 1.0^{ad}	
Estimated $m\dot{V}O_2$ ($\mu M/g/min$)	14.8 ± 0.7	89.0 ± 35.7^d	126.3 ± 22.5^{ad}	142.9 ± 14.8^{ad}	
Estimated $\Delta m\dot{V}O_2$ ($\mu M/g/min$)	–	74.2 ± 35.6	111.5 ± 21.9^a	128.1 ± 14.4^a	

7

8 Values are mean \pm SD (n = 6). $m\dot{V}O_2$ and $\Delta m\dot{V}O_2$ was measured using O_2 electrodes. Both
9 microvascular and intracellular $[O_2]$ were calculated as values equilibrium with $P_{cap}O_2$ and
10 $P_{mb}O_2$, respectively (microvascular or intracellular $[O_2] = (P_{cap}O_2 \text{ or } P_{mb}O_2) \times O_2 \text{ solubility}$.
11 The O_2 solubility is $0.00135 \mu mol/ml/mmHg$ at $37^\circ C$ (Philip and Dorothy, 1971)). The O_2
12 gradient represents the difference of $[O_2]$ between microvasculature and myocyte. The
13 estimated $m\dot{V}O_2$ was calculated by multiplying O_2 gradient and flow rate. $\Delta m\dot{V}O_2$ stands for
14 net increase in $m\dot{V}O_2$ due to contraction. The superscripts indicate significant difference (a; vs.
15 50%, b; vs. 75%, c; vs. 100%, d; vs. Rest, $p < 0.05$).

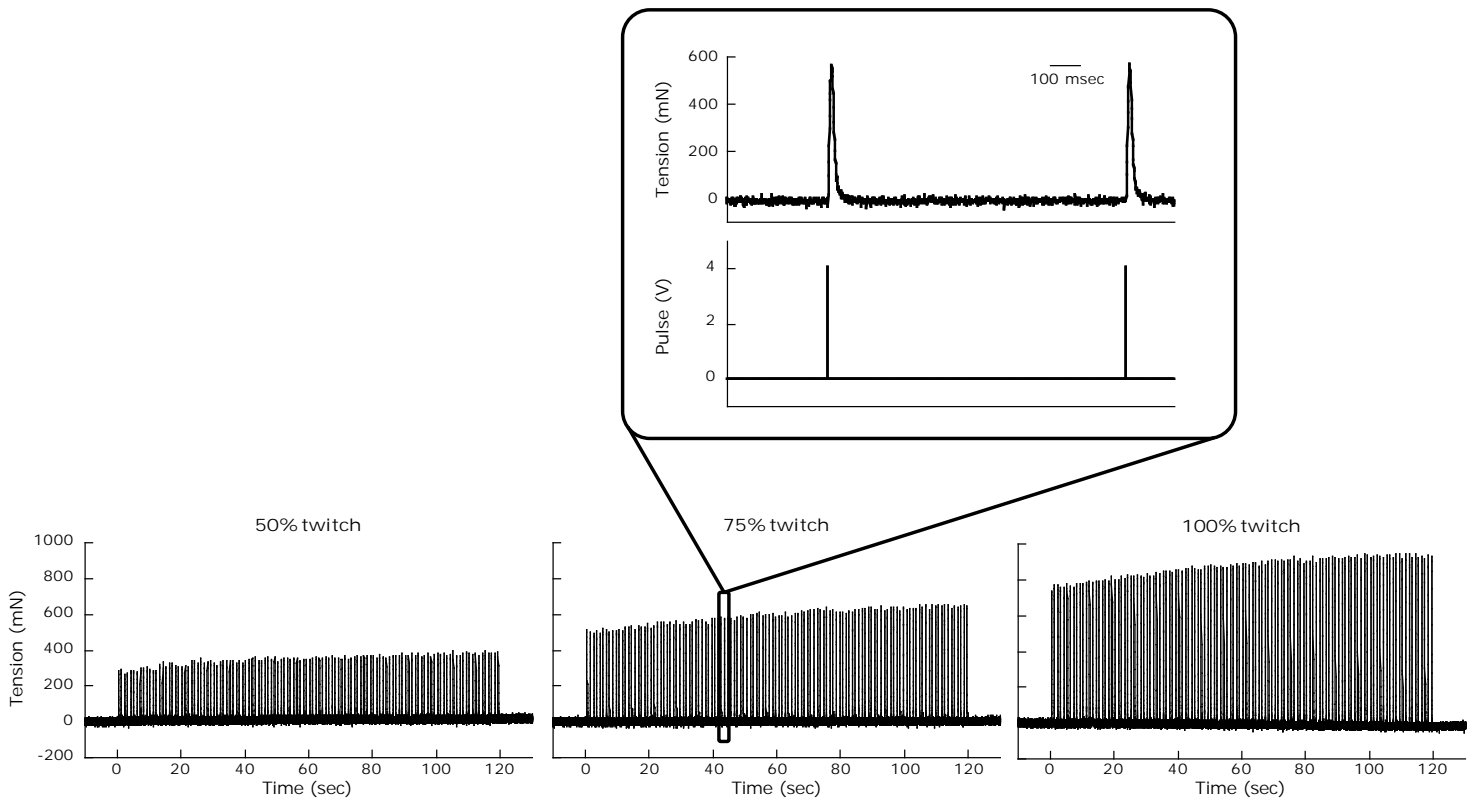


Figure 1

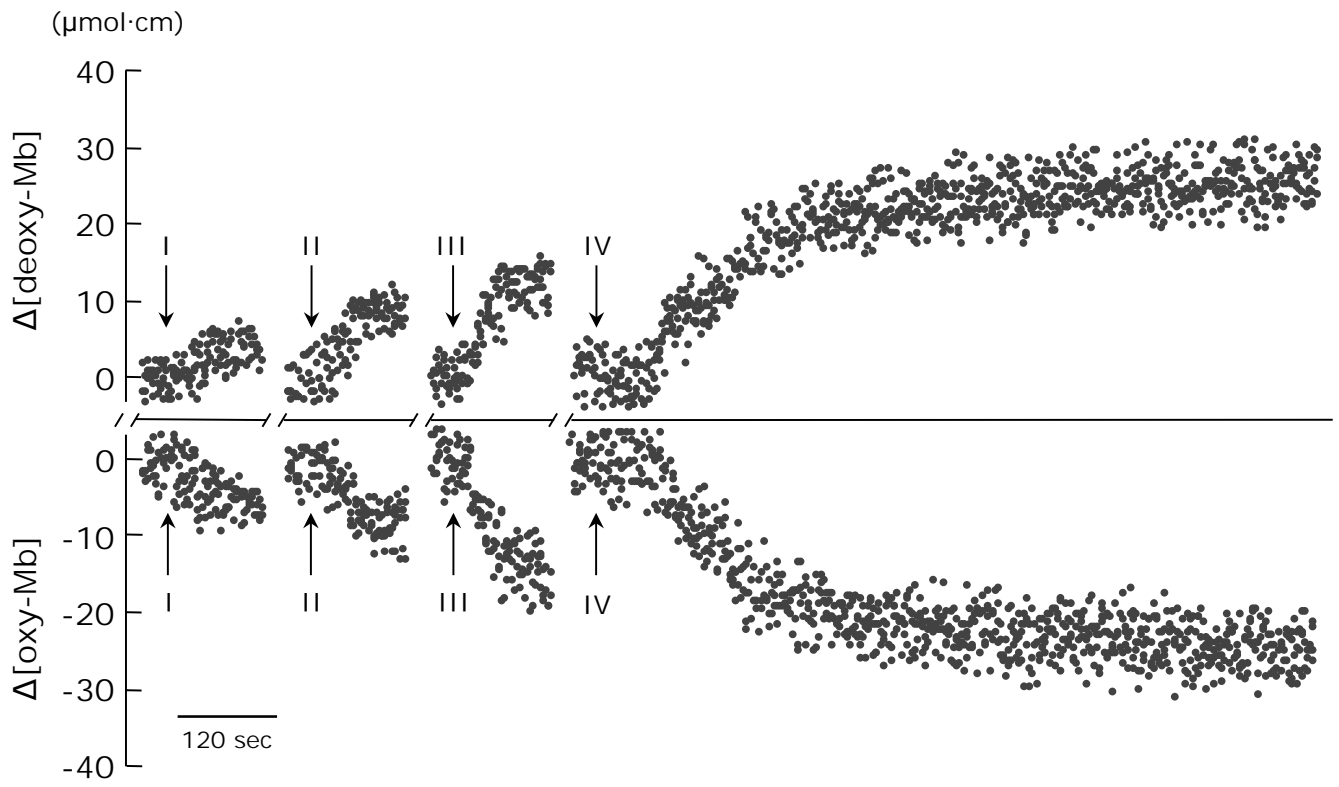


Figure 2

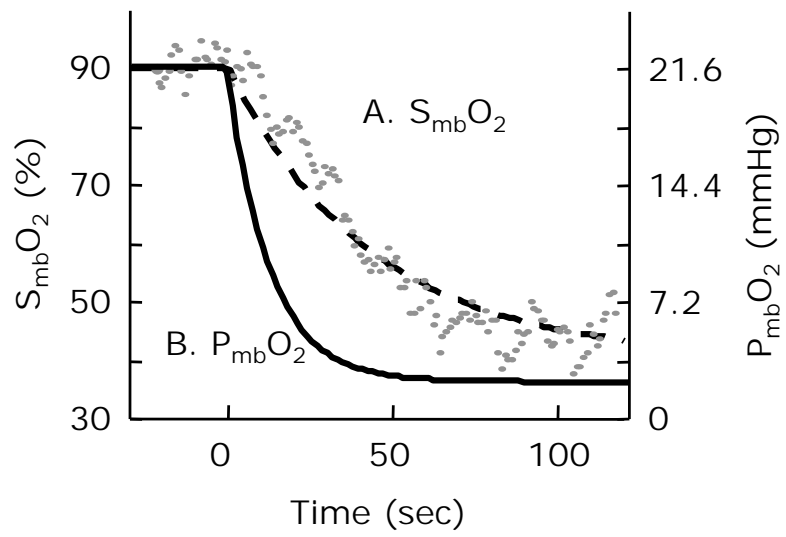


Figure 3

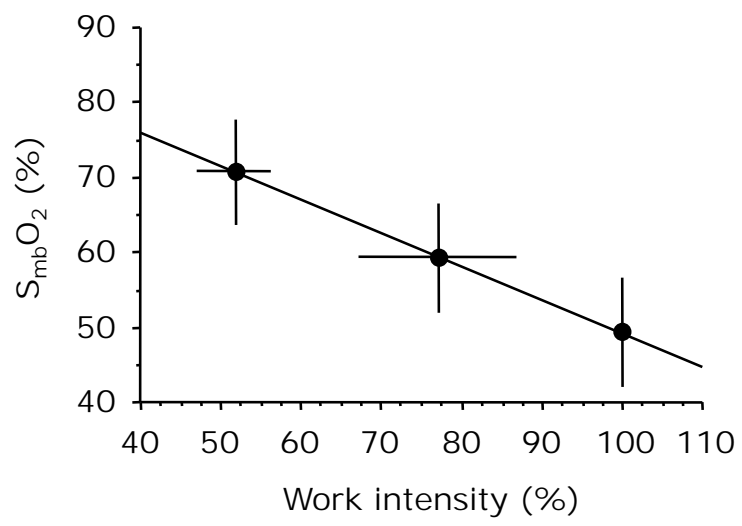


Figure 4

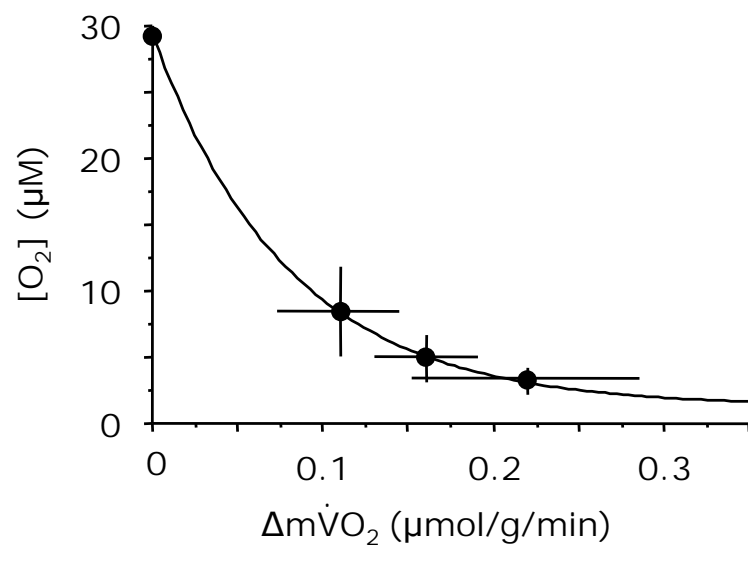


Figure 5

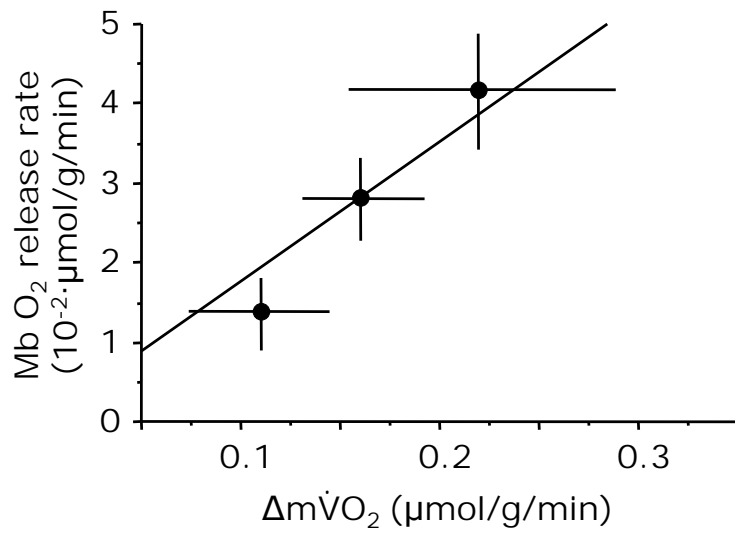


Figure 6